Science Advances
AAAS

Supplementary Materials for

Mechanics of colloidal supraparticles under compression

Junwei Wang, Jan Schwenger, Andreas Ströbel, Patrick Feldner, Patrick Herre, Stefan Romeis, Wolfgang Peukert, Benoit Merle, Nicolas Vogel*

*Corresponding author. Email: nicolas.vogel@fau.de

Published 13 October 2021, *Sci. Adv.* **7**, eabj0954 (2021)
DOI: 10.1126/sciadv.abj0954

The PDF file includes:

Figs. S1 to S9

Other Supplementary Material for this manuscript includes the following:

Movie S1

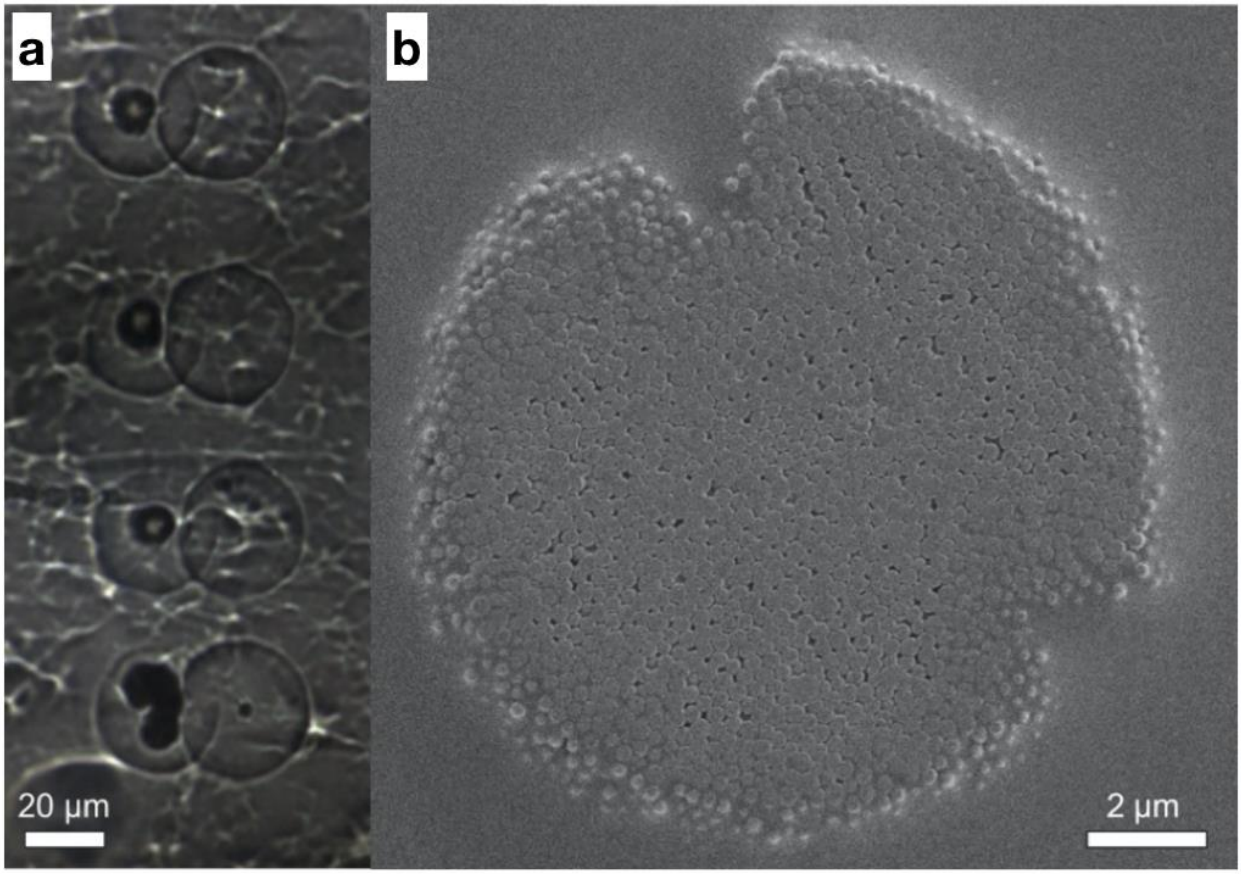

Fig. S1, Procedure to clean the indentation tip. After each indentation measurement, the fractured supraparticle or its fractured pieces can adhere to the tip, which impedes the accuracy of the next measurement. To clean the tip, after each measurement, the tip is moved to a double-sided scotch tape and two consecutive indentations are performed into the tape. (**A**) shows four successful cleaning procedures. The tip first indents into the tape and leaves the adhered supraparticles or any fractured parts. A circular mark which shows the size of the tip is much larger than the supraparticle (left parts). The tip then indents again into another position in the tape to make sure it is free of any particles. In all cases, the second indentation did not show any remaining supraparticle pieces, indicating that the procedure is effective. (**B**) shows a fractured supraparticle immersed in the polymer adhesives of the tape from (**A**).

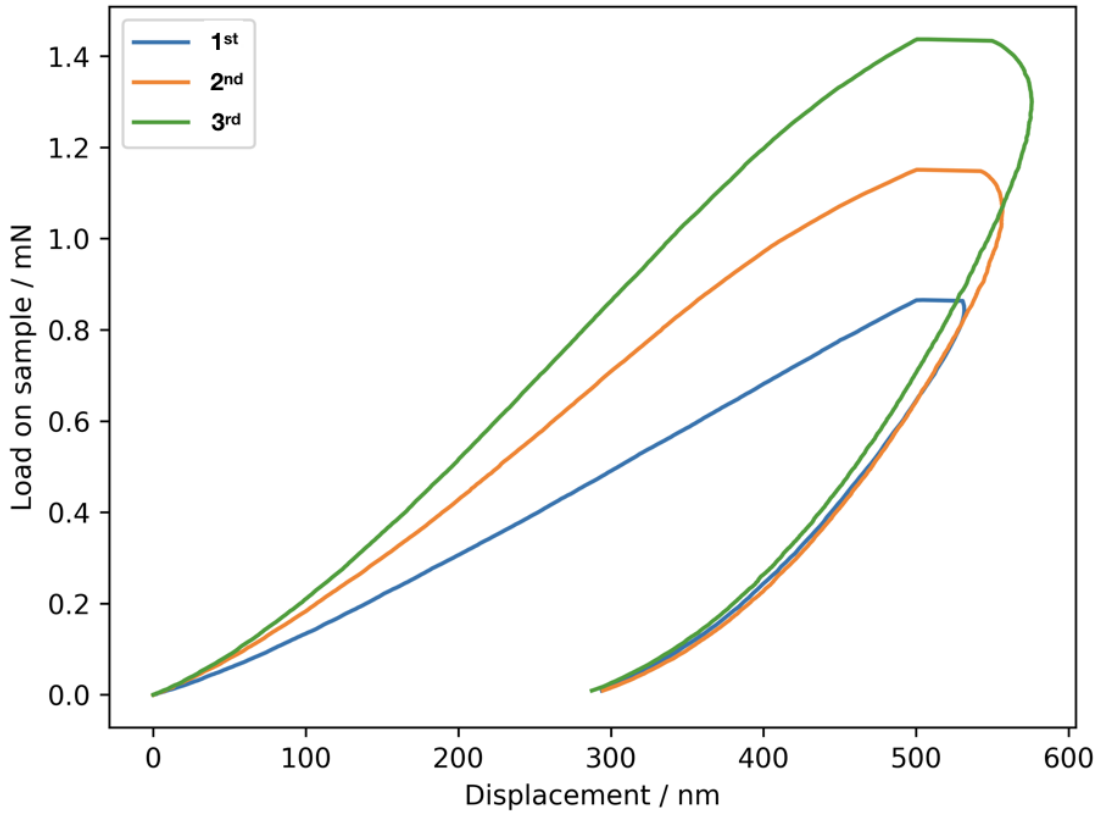

Fig. S2, Consecutive indentations into one supraparticle. After each compression (500 nm displacement into the supraparticle, diameter of 10 µm, 244 nm PS primary particles), the deformation resistance of the sample increases, possibly due to densification and larger contact area due to deformation. The creep also increases. The unloading curves overlaps, suggesting the stored elastic deformation of supraparticles remains similar after cyclic loading. The EPL increases after each loading, indicating that the sample is becoming more plastically deformed.

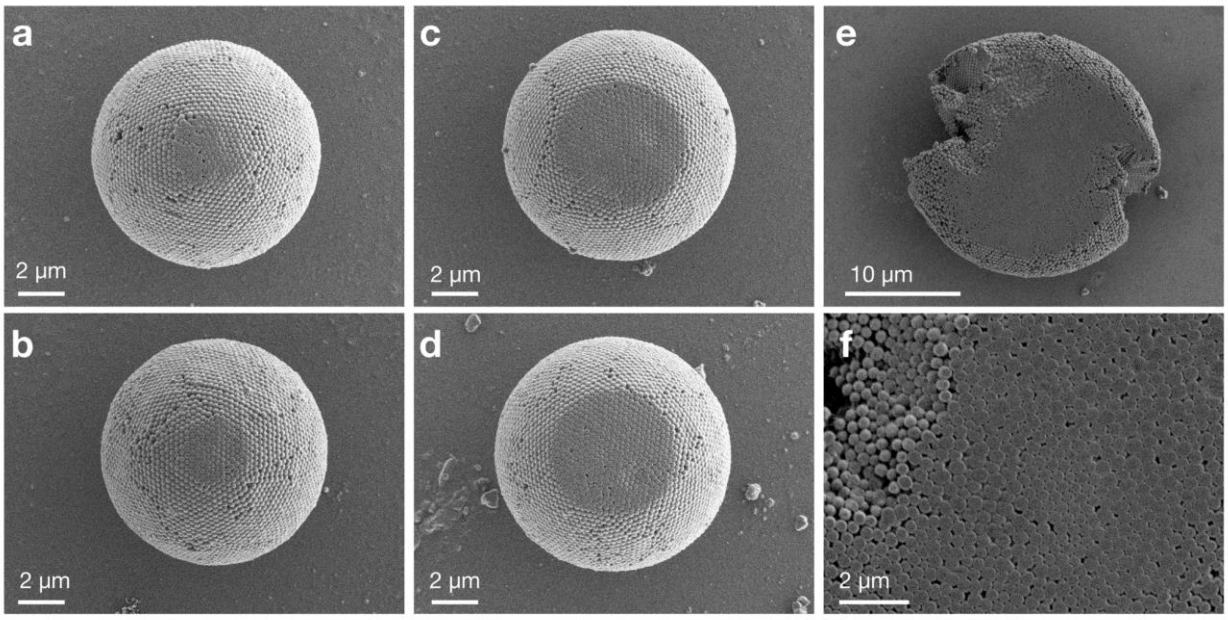

Fig. S3, Deformation of PS primary particle with small (**A**,**B**), medium (**C**,**D**) and large strain (**E**,**F**) in ambient condition. These corresponds to Fig. 2A and Fig. 2B. Note that despite large crack formation and shape changes, the supraparticles compressed in ambient condition remained as one piece (**E**). (**F**) shows that the interstitial spacing between the primary particles is significantly reduced in the contact area due to large primary particle deformation.

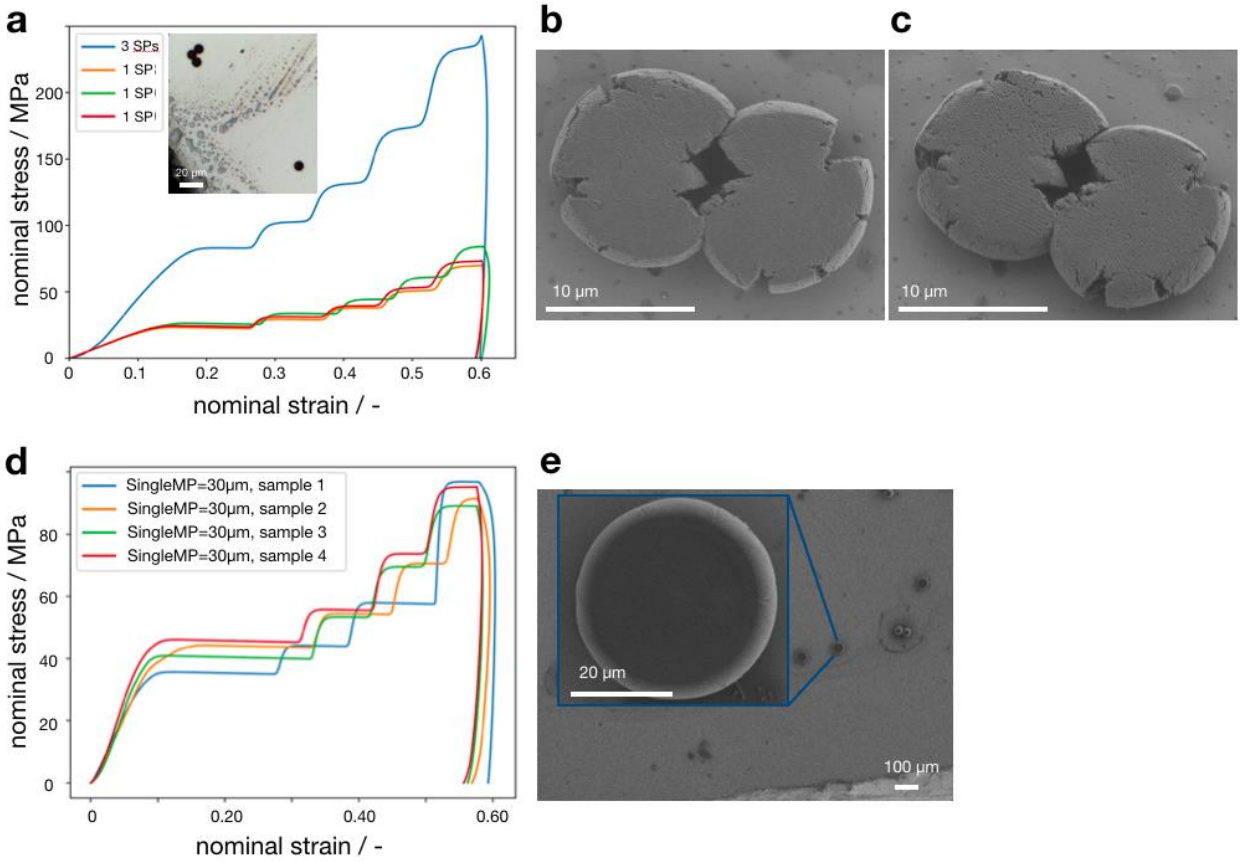

Fig. S4, Additive mechanical response of supraparticles. (**A**) The nominal stress-strain curve (blue) of three adjacent supraparticle compressed together takes the same shape as individual supraparticle curves (SP = 10 µm, PP = 244 nm at 48% humidity) but is magnified in stress a bit more than three-fold. (**B** and **C**) Deformation of two supraparticles compressed together, viewed at different angles. Multiple cracks are visible at the periphery. The contact between two supraparticles explain the slight increase in the total stress than the combination of individual supraparticles. (**D**) Multiple fracturing during compression of single large PS microsphere, similar to the compression behavior of PS supraparticles in Fig. 2B. This indicates that the supraparticle in ambient condition behaves generally similar to single PS microspheres. Note that the data for single microspheres show a slightly larger scatter compared to the supraparticle sample. This may be related to a more uniform defect distribution of supraparticles: since the SPs are held together by contacts between primary particles, one can consider them to consist entirely of defects (or a network of defects). In contrast, plain single microspheres may exhibit a more random distributions of defects. (**E**) Plastic deformation of single large PS sphere of 30 um. Three deformed and flatten spheres after indentation measurement can be seen on the substrate, compared to two undeformed spheres. Despite the similarity to supraparticle in the stress-strain curve, large PS sphere does not exhibit large open cracks at the periphery but shallow pleats.

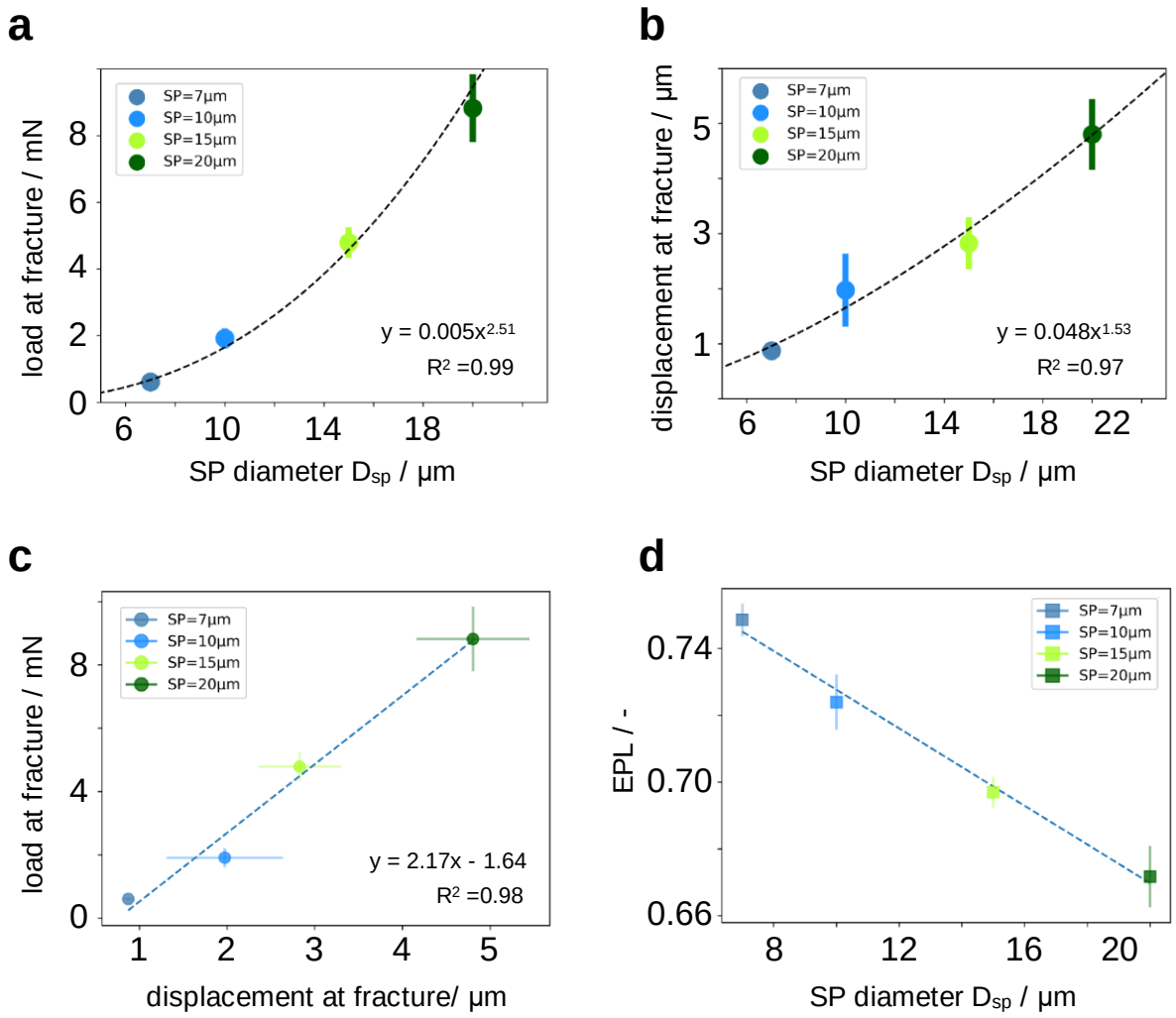

Fig. S5, Scaling relationship between mechanical properties and supraparticle geometry. (**A**) The load at fracture of supraparticles scales with the supraparticle diameter with a 2.5 power law. The error bar represents the standard deviation. The supraparticle diameter is taken from batch samples fabricated by microfluidics, showing less than 1 µm deviation. Individual supraparticle diameter were not measured for each indentation, therefore no deviation in the supraparticle diameter is available. (**B**) The displacement at fracture of supraparticles scales with the supraparticle diameter with a 1.5 power law. (**C**) The load at fracture scales linearly with the displacement at fracture for supraparticles. Here, the deviation in the displacement is directly available from the indentation measurement. (**D**) The elastic-Plastic-Loading index decreases linearly with supraparticle diameters.

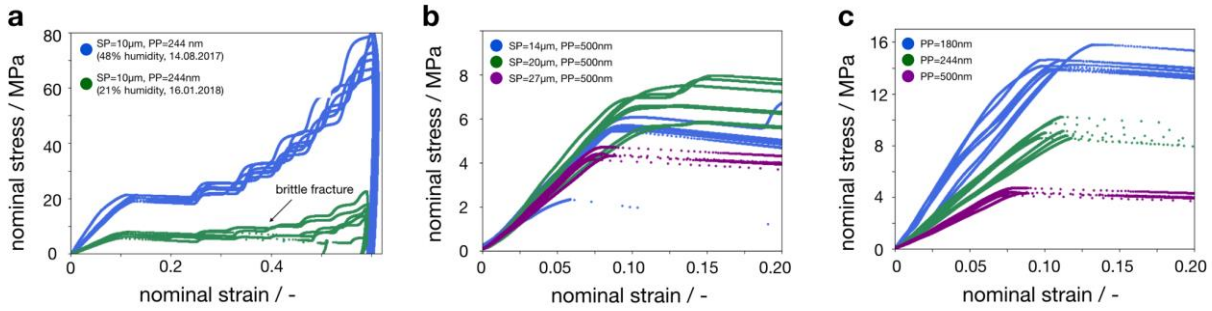

Fig. S6, Effect of humidity on the mechanical behavior of supraparticles under compression. (**A**) The same supraparticle sample (consisting of 244 nm PS PPs) measured at different humidity (summer 48% humidity and winter 21% humidity). Reduced humidity causes a reduction in deformation resistance and a change of fracture mode from ductile to brittle. (**B**) Deformation resistance of supraparticles (i.e. the slope of the nominal stress vs nominal strain curve) is independent of their sizes in reduced humidity (20%). All individual measurements are shown together. The diameter of PS PPs is 500 nm. The nominal stress- nominal strain curves collapse, but the fracture points no longer correlate with supraparticle size (as in Fig. S4). The fracture becomes more brittle, indicated by separated dots (each a recorded value of load and displacement) as the sample fracture apart quicker than the advancement of tip, not seen in the supraparticles measured in higher humidity (Fig. 2 and Fig. 3). (**C**) In reduced humidity (20%), the deformation resistance of SPs increases with decreasing PP diameter (blue: PP = 180 nm, SP = 11 µm; green: PP = 244 nm, SP =14 µm; purple: PP = 500 nm, SP = 27 µm), similar to the case of higher humidity (Fig. 2). However, the SPs exhibit a change in fracture mode to a brittle fracture, indicated by separated dots. The change from ductile to brittle fracture mode is more apparent with increasing PP diameter, indicated by the dispersed data points in each measurement when the indenter tip records no resistance from the sample until further displacement.

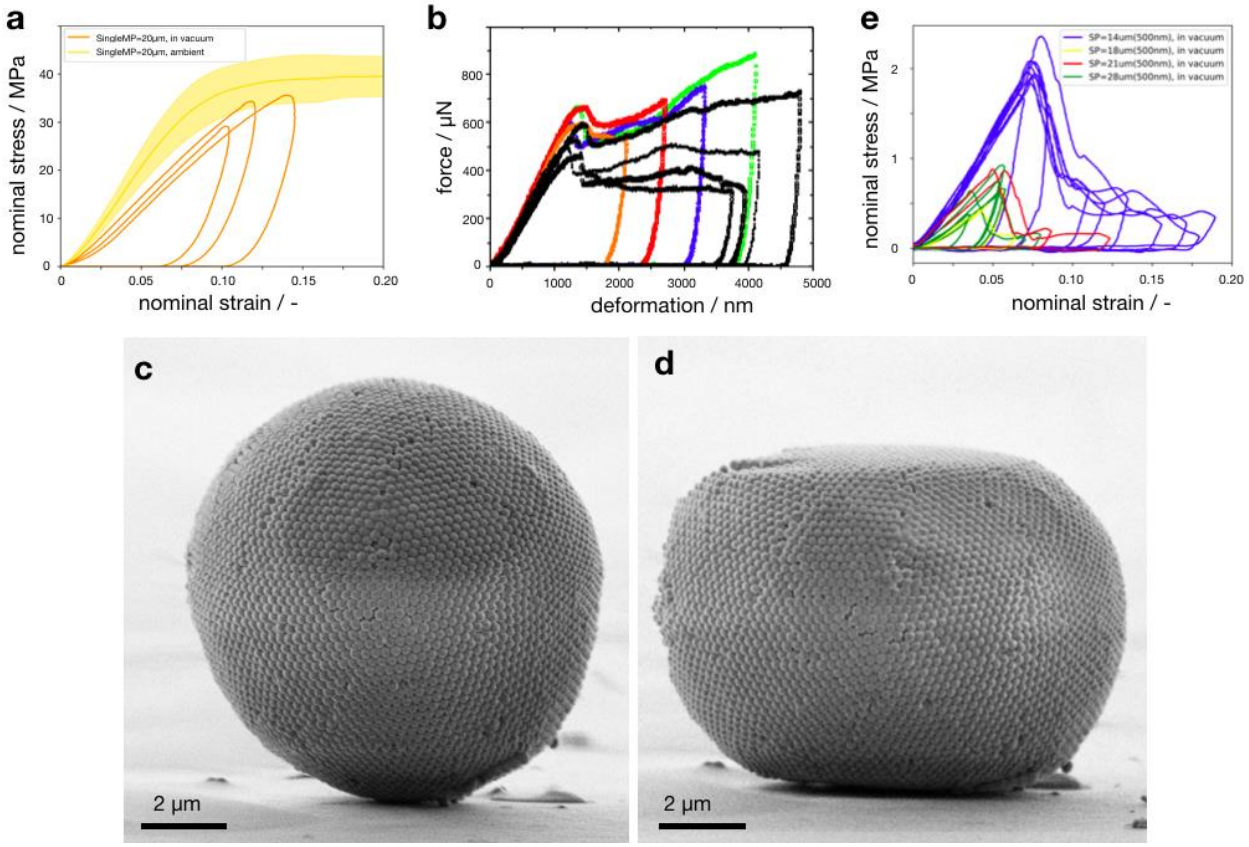

Fig. S7, PS supraparticles under compression in vacuum. (**A**) A single large (20 µm) PS microsphere show similar deformation resistance, the nominal stress and strain at first fracture point in both ambient condition and in the high vacuum of the SEM. (**B**) Effect of electron beams on the mechanical response of supraparticles is negligible. Force and displacement recorded with electron beams switched on inside the SEM chamber during the compression experiment (black) are similar to those recorded without electron beam (colored). (**C**) PS supraparticles before compression. (**D**) PS supraparticles after compression in vacuum. The crack formed during the compression is only barely visible to the left side of the supraparticles. Except for the upper and lower surface that was in direct contact with the indenter tip, the surface does not show relative particle rearrangements. (**E**) Nominal stress-strain curve for supraparticles in vacuum (PP = 500 nm). The deformation resistance is no longer uniform for different supraparticles diameters.

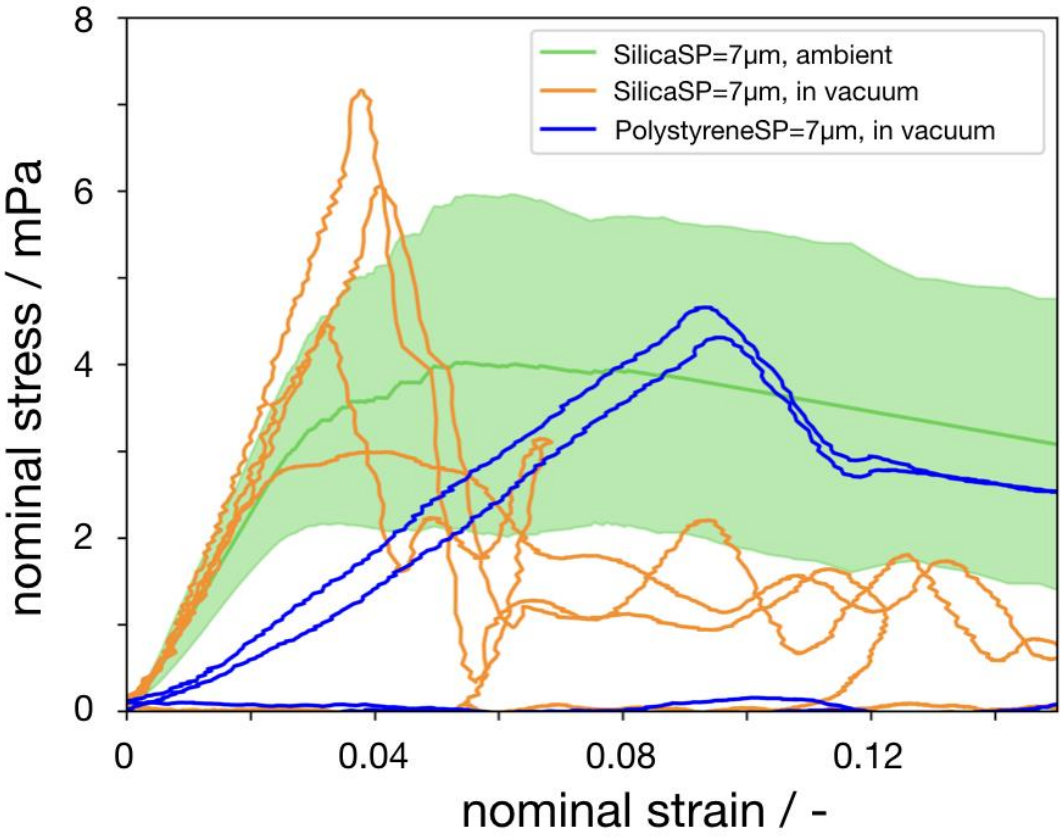

Fig. S8, The deformation resistance of silica supraparticles in ambient humidity and in vacuum remain the same.

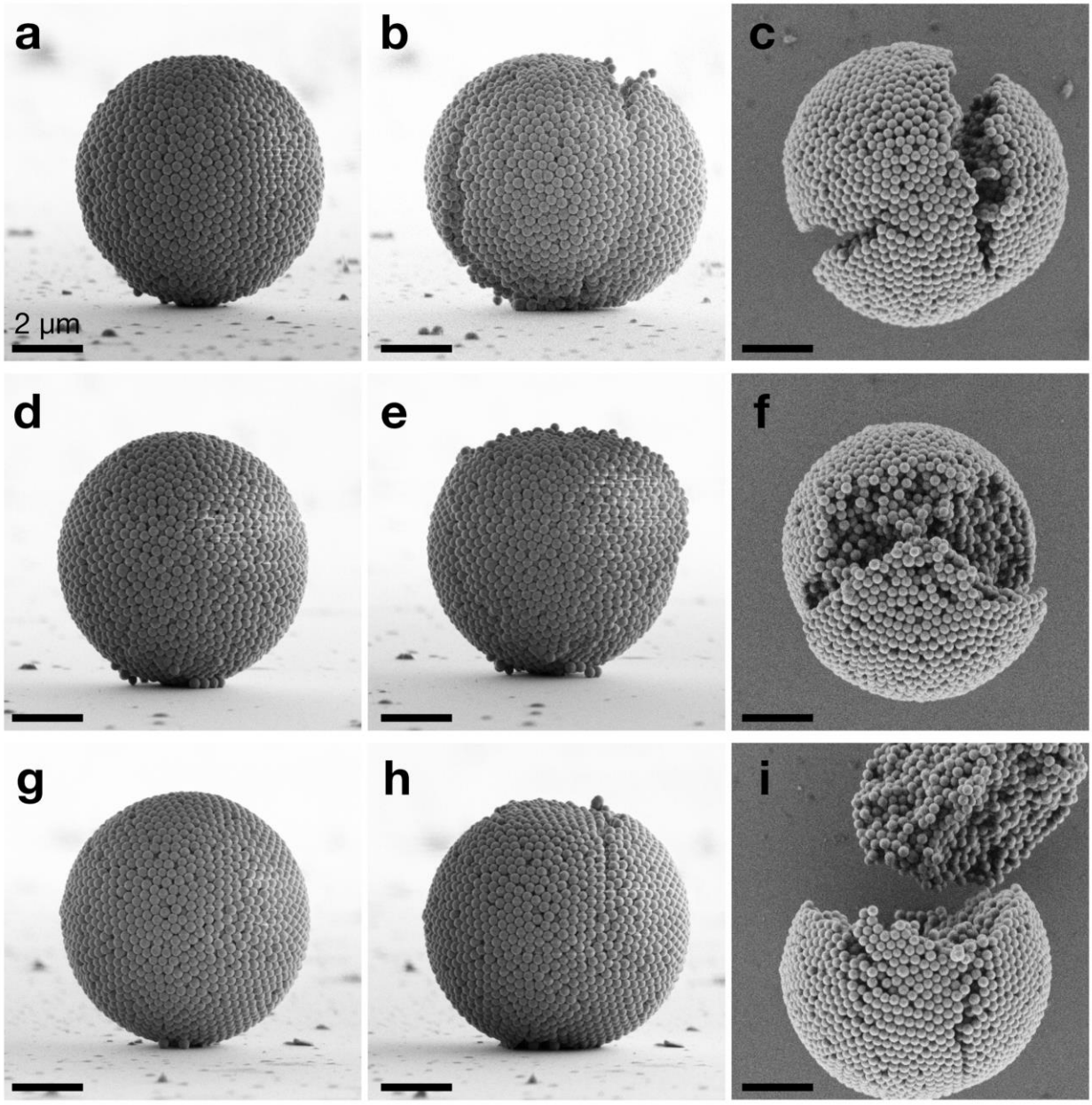

Fig. S9, Three silica supraparticles before (**A**,**D**,**G**) and after compression in vacuum (**B**,**E**,**H** for side view, **C**,**F**,**I** for top view). Notice that individual primary silica particle shows no visible deformation, and the supraparticle fracture in a brittle way into several pieces while PS supraparticles remain as one piece (Fig. 2).